

ITALIAN SUMMER PROGRAM AT FERMILAB

UNIVERSITÀ DEGLI STUDI DI BARI

Designing the Neutron Detector for the NEXUS Test Facility

Student: Paola Mastrapasqua

Supervisor: Patrick Lukens, Lauren Hsu

October 12, 2019

Abstract

The SuperCDMS dark matter experiment is commissioning a new test facility at Fermilab, NEXUS, capable of testing a new suite of detectors that promise to push to lower dark matter masses than has previously been achieved. These detectors use silicon and germanium, cooled to tens of mK, to measure small vibrations in the crystal lattice caused by very tiny energy deposits.

A core capability of NEXUS test facility is to use a commercial neutron generator, coupled to an array of detectors behind the test facility, to calibrate the nuclear recoil energy scale of these detectors through neutron scattering. The response of silicon and germanium to nuclear recoils below 1 keV energy transfer is largely unknown. For dark matter models which are primarily interacting with the nucleus, calibration of this response will completely determine the dark matter sensitivity of the experiment.

In this context, the proper design of the neutron tagging detector to be used in the test facility needs to be found. This work will include simulation of the detector behavior and work towards an optimization of the detector geometry based on measurement resolution and detection rate. In addition, prototype scintillators and photodetectors will be studied as candidate detector elements.

1 SuperCDMS experiment

According to models of cosmological structure formation, the luminous matter of galaxies is gravitationally bound to a more massive halo of dark matter. If the dark matter of the universe consist of unidentified particles, our solar system and our planet would be passing through a flux of these dark matter particles which constitute the dark halo of the Milky Way galaxy.

These dark matter particles could be detected directly using sensitive detectors located in underground laboratories, to shield them from interactions from normal matter particles. Such dark matter interactions would deposit a small, but measurable, amount of energy in an appropriately sensitive detector by elastically scattering from nuclei.

SuperCDMS is a next-generation experiment designed to search for low-mass dark matter particles ($\lesssim 10 \text{ GeV}/c^2$) through this kind of direct detection. It will use two types of detector (HV and iZIP) and two types of target materials (Silicon and Germanium) to detect crystal lattice vibrations (phonons) and ionization (charge) generated within the detector crystal by elastic collisions between detector nuclei and dark matter particles. The two types are somewhat complementary: HV detectors have a better sensitivity for mass $\lesssim 5 \text{ GeV}/c^2$ and have only phonon sensors, while iZIP detectors have a better sensitivity above $\sim 5 \text{ GeV}/c^2$ and have both phonon and ionization sensors (see **Figure 2** for information about expected sensitivity).

Moreover the facility will include a cryogenics system designed to maintain the detectors at temperatures within a fraction of a degree above absolute zero in order to damp out thermal noise. This will be surrounded by layers of clean shielding materials to exclude radioactive backgrounds from the environment.

A crucial part of the experiment is the calibration since, in order to perform measurements, it is necessary to know the relationship between the detector signal and the actual energy released by dark matter particle scattering (**Figure 3**). The relationship between the total phonon energy (E_{total} , which is extracted from the detector output signal) and the recoil energy (E_r) is given by:

$$E_r = \frac{E_{total}}{1 + Yield \frac{eV_{bias}}{\varepsilon}} \quad (1)$$

where e is the electron charge, V_{bias} is the bias voltage chosen for the detector, ε is the mean energy required to create an electron-hole pair (3.0 eV in Ge and 3.82 eV in Si), and $Yield$ is the ratio between $E_{ionisation}$ and E_r . It is measured directly in the case of iZIP, while for HV it must be determined independently in order to extract the recoil energy [2].

A way to calibrate the nuclear recoil energy scale is to use a neutron scattering setup, and that's

the reason why NEXUS facility was commissioned.

The measurement of the yield is also important because there are no previous studies of this type at the low energies (≤ 1 keV) the SuperCDMS is interested in. **Figure 1** shows previous experiment data for measurement of the ionization yield in Si, compared with the theoretical prediction (Lindhard theory). The measurements disagree with the prediction and the data indicate a lower yield. Since the trend shows a large deviation from experiment at low energies, it is naturally very interesting to measure the ionization yield down to ~ 100 eV where SuperCDMS (and NEXUS) will operate [1].

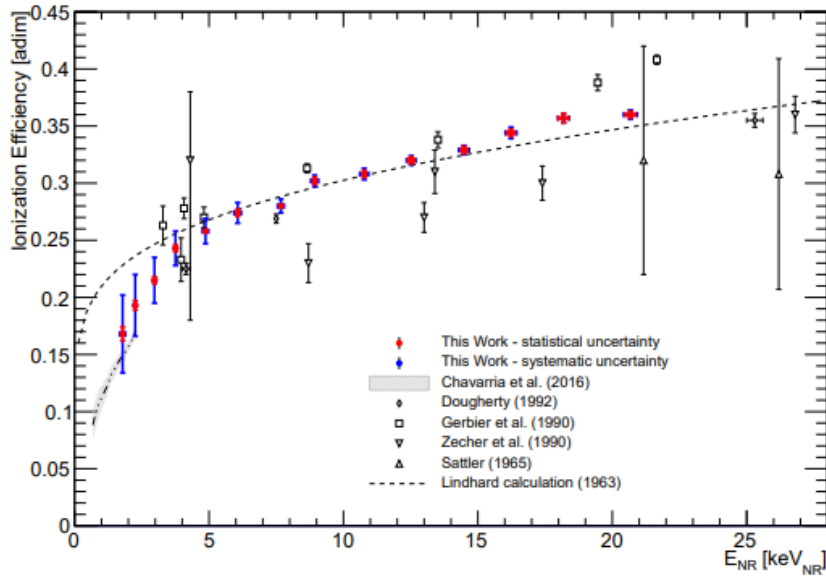


Figure 1: Yield as a function of the nuclear recoil energy. The points are experimental data while the dashed curve is Lindhard prediction for silicon [1].

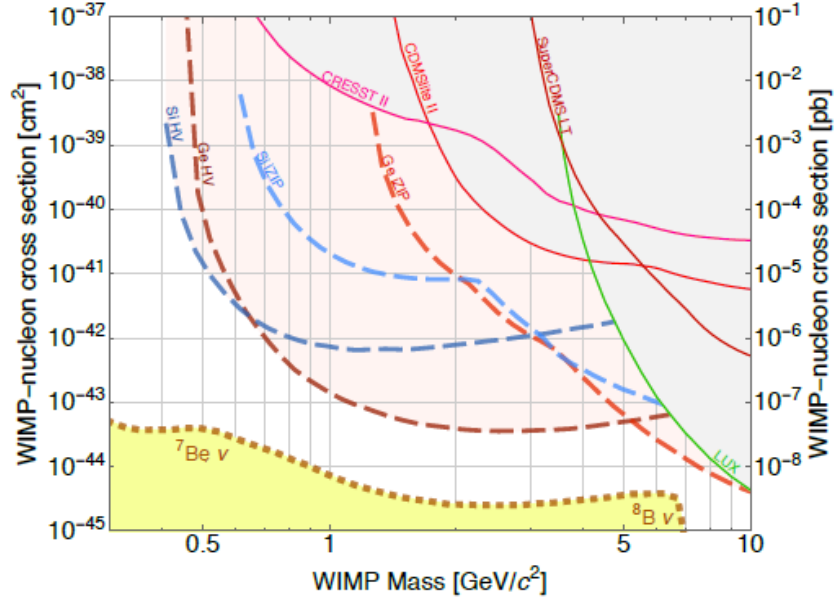


Figure 2: Projected exclusion sensitivity for the SuperCDMS SNOLAB direct detection dark matter experiment. The vertical axis is the spin-independent WIMP-nucleon cross section under standard halo assumptions, and the horizontal axis is the WIMP mass, where WIMP is used to mean any low-mass particle dark matter candidate. The blue dashed curves represent the expected sensitivities for the Si HV and iZIP detectors and the red dashed curves the expected sensitivities of the Ge HV and iZIP detectors. The solid lines are the current experimental exclusion limits in the low-mass region, from the CRESST-II, SuperCDMS and LUX experiments. The dotted orange line is the dark matter discovery limit, which represents the cross-section at which the interaction rate from dark matter particles becomes comparable to the solar neutrino coherent elastic scattering rate [2].

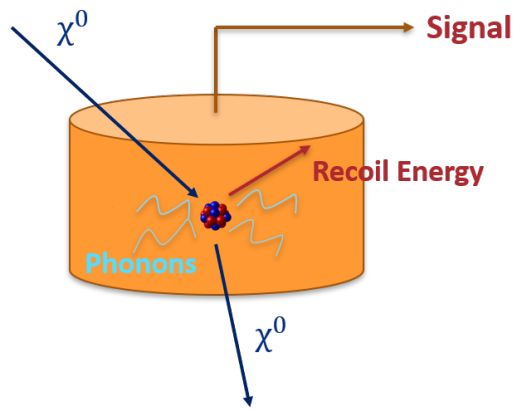


Figure 3: Simplified elastic collision between detector nucleus and dark matter particle χ^0 .

2 NEXUS Facility

The calibration setup is shown in **Figure 4**.

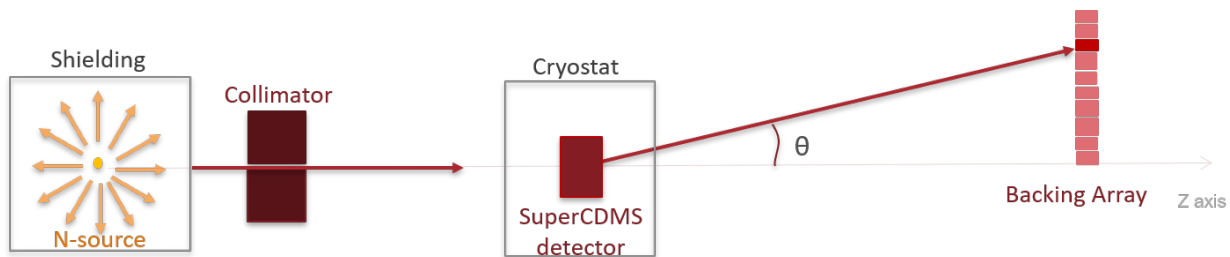


Figure 4: NEXUS facility: calibration setup.

The neutron source is a D-D generator which produces isotropically approximately 10^8 *neutrons/s* with an energy of 2.45 MeV. The collimator selects a flight direction, creating a more or less collimated neutron beam directed towards the target. Some of the neutrons that hit the SuperCDMS detector in the cryostat interact with Si/Ge nuclei, scatter and are detected by the Backing Array. The Backing Array will be made of many units of bunches of 2-3 scintillating fibers wound to form a ring and coupled to two Silicon PhotoMultiplier (SiPMs) at the two ends. Every unit covers a small range in terms of scattering angle, so that knowing which unit fires implies measuring the scattering angle with a certain error. Through Eq.2, it is possible to determine the nuclear recoil energy from the measurement of the scattering angle, thus calibrating the SuperCDMS detector that measures the total phonon energy related to the same scattering event. Of course, the better is the angle resolution, the better is the energy resolution, the better is the calibration.

$$E_r(\theta) = 2E_n \frac{M_n^2}{(M_n + M_t)^2} \left(\frac{M_t}{M_n} + \sin^2 \theta - \cos \theta \sqrt{\left(\frac{M_t}{M_n} \right)^2 - \sin^2 \theta} \right) \quad (2)$$

where E_n is the initial neutron energy (2.45 MeV), M_n is the neutron mass, M_t is the target nucleus mass, and θ is the scattering angle.

3 Designing the Backing Array: Simulation

As previously described, the Backing Array (B.A.) will be made of scintillating fibers coupled with SiPMs. The purpose of this study is to find the proper geometry for this detector in order to achieve at the same time high rate and good resolution for the energies of interest. As the experiment is searching for low mass dark matter particles, the range of interest goes from 50 eV (for the lightest dark matter we are sensitive to) to 1 keV.

Before designing the geometry of the detector, it is important to estimate the systematic uncertainty related to the finite size of source, collimator and target, in order to not overdesign the detector

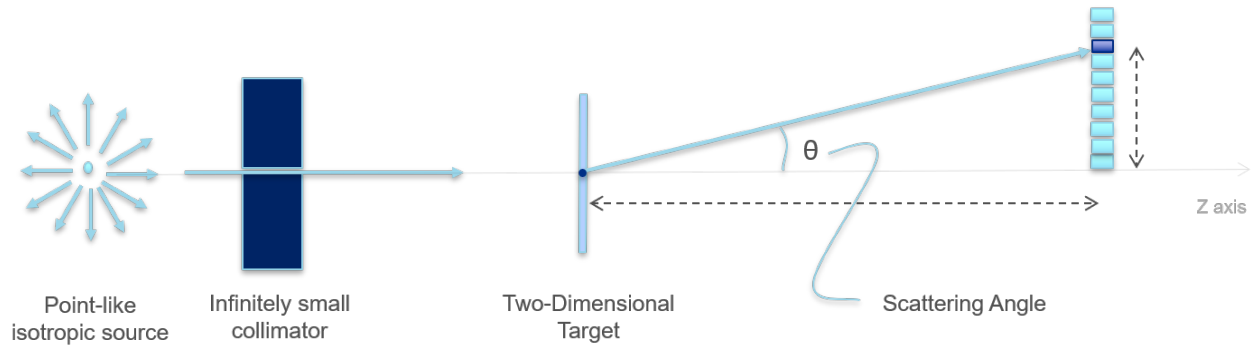


Figure 5: Ideal scattering

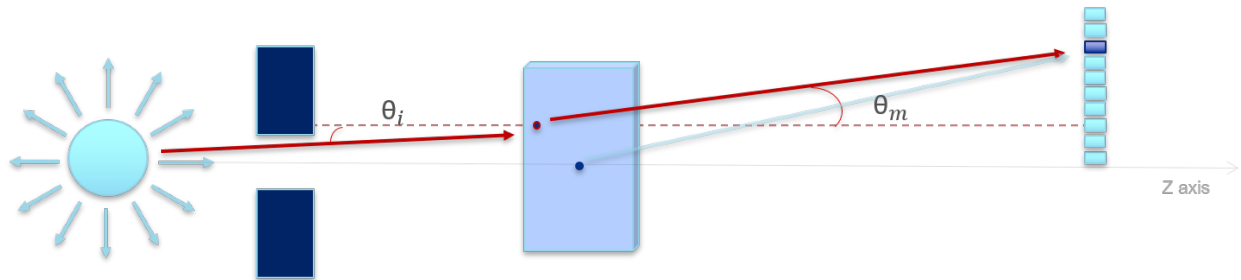


Figure 6: Real scattering

itself. Thus the first step is neglecting the uncertainty due to the finite size of the B.A. and evaluate the best theoretical precision it is possible to obtain, considering the impossibility to constraint the scattering point inside of the target better than the collimator size and the target thickness.

3.1 Systematic Uncertainty

Figure 5 shows an ideal scattering experiment: since the scattering point in the target is known without uncertainty, θ is absolutely known (assuming a point-like detector). Nevertheless, in a real scattering experiment, both the source and the collimator have a finite size and the target has a non-infinitesimal thickness, so that the scattering point is not absolutely known, as well as the incident angle (**Figure 6**).

In order to estimate the error on the angle measurement that occurs approximating the scattering point with the center of the target, a geometrical Monte Carlo is performed. The ROOT code implements the random generation of particles inside of a sphere (the neutron source) and their emission in a random direction. Considering the collimator only as a geometrical constraint, the scattering point inside of the target is found: the position in the flight direction is randomly extracted from a truncated exponential(Eq.3), while the position on the orthogonal plane is simply calculated from trigonometry considerations (**Figure 7**).

$$P(z) = \frac{1}{\lambda} e^{-z/\lambda} \left(1 - e^{-t/\lambda}\right)^{-1} \quad (3)$$

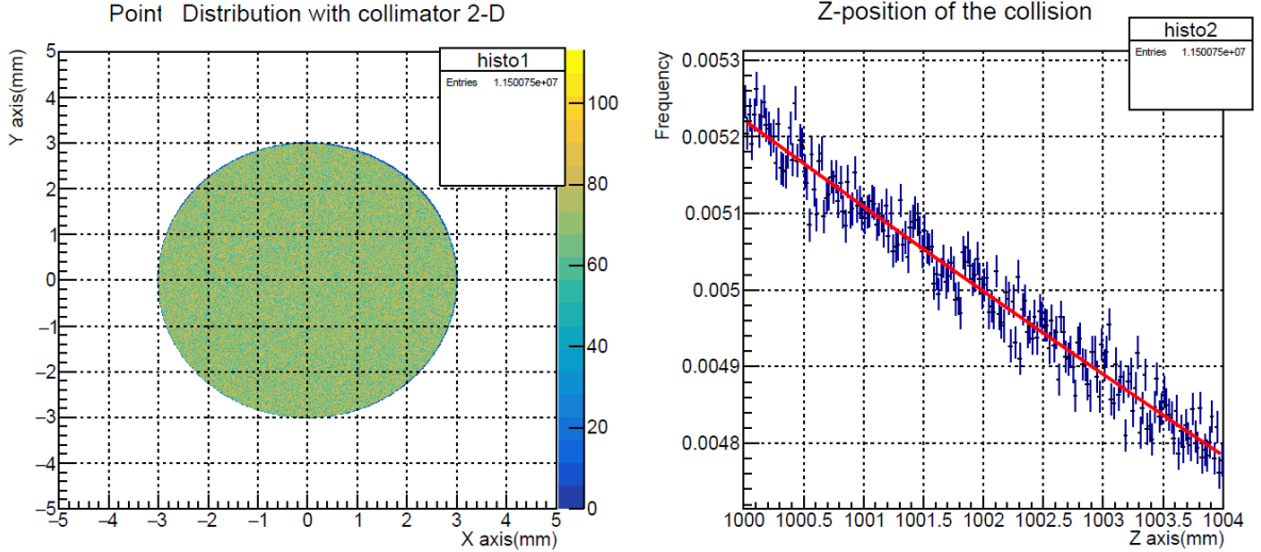


Figure 7: Simulated collision points at target in xy plane (plane orthogonal to flight direction) and in the z direction (flight direction). The coordinate system origin is fixed in the n-source center. In this simulation, the target is placed at 1m distance from the origin and it's 4 mm thick, while the collimator has a 3mm-radius.

Source Radius	1 mm
Collimator Radius	3 mm
Source-Target distance	1 m
Target-Detector distance	2 m
Detector size (Small one)	1 cm * 1 cm * 0.4 cm

Table 1: Default parameters

where λ is the interaction length in Si(50 mm)/Ge(65 mm), z is the depth into the target and t is the target thickness.

Once the collision points are obtained, the ideal scattering angle θ_{ideal} is evaluated by inverting Eq.2 for recoil energy of 50, 100, 200 and 1000 eV (E_r). From θ_{ideal} , it is possible to extract the B.A. detector that fires (for now, supposing it is point-like) and for each collision point evaluate θ_{real} . Finally from Eq.2, E_{real} is evaluated. The histogram of $(E_r - E_{real})/E_r$ gives an idea of the energy resolution.

This first part of the study is independent from the geometrical properties of the B.A., since it is supposed to be pointlike. The setup default parameters are shown in **Table 1**. They represent the best can be experimentally achieved. Different studies are performed by varying separately one parameter at time, in order to understand the influence of the parameter on the energy resolution (Results in Sec.4).



Figure 8: Simplified representation of the B.A. geometry and an expanded view of one of its units.

3.2 Implementation of the Detector Geometry

In the second part of this simulation study, the detector geometry is implemented into the code (**Figure 8**). The B.A. is composed of concentric rings made by bunches of fibers wound together. Each ring-like unit has a thickness Δr and a length L in the z direction. These two parameters are changed separately in order to understand the dependence of the energy resolution on these values (Results in Sec.4).

4 Simulation & Analysis Results

All energy histograms are shown in Appendix A. For every histogram the Cumulative Distribution Function (CDF) is evaluated. Through this function, σ_1 and σ_2 are found in terms of $\Delta E/E$: they are determined in such a way that the 68.27% of values lie in the range $[\sigma_1, \sigma_2]$. Thus, σ_1 and σ_2 offer a way to compare quantitatively the results.

Table 3 is a comparative table for different studies: only the specified parameter is changed; the others are taken equal to the default ones. The simulation results show that the crucial point in the setup is the collimator radius, since as it doubles also the resolution doubles. On the contrary, target and detector thickness does not affect a lot the spread of the histogram, and also Δr has a small influence as it remains less then $R_{collimator} * dist_{source-detector} / dist_{source-target}$.

In general, it is evident that the uncertainty in the z -direction has a smaller influence on the energy resolution than the uncertainty in x and y direction. This is definitely a good news, since it is possible to increase the length of the detector and so the detection probability and the event rate, without worsening the precision.

To sum up the results, **Table 2** shows the theoretical best resolution is possible to achieve at fixed energy.

50 eV	100 eV	200 eV	1 keV
$\sim 24\%$	$\sim 17\%$	$\sim 12\%$	$\sim 5\%$

Table 2: Best possible resolution for different recoil energies.

POINT-LIKE				
Default parameters				
	50 eV	100 eV	200 eV	1 keV
σ_1	0.237	0.164	0.114	0.050
σ_2	0.195	0.142	0.102	0.046
3 mm source radius				
	50 eV	100 eV	200 eV	1 keV
σ_1	0.260	0.179	0.124	0.054
σ_2	0.208	0.151	0.109	0.050
6 mm collimator radius				
	50 eV	100 eV	200 eV	1 keV
σ_1	0.511	0.345	0.235	0.100
σ_2	0.352	0.265	0.194	0.091
Big detector: $3.3 * 10 * 10 \text{ cm}^3$				
	50 eV	100 eV	200 eV	1 keV
σ_1	0.213	0.143	0.095	0.036
σ_2	0.205	0.153	0.116	0.065

3-D				
$\Delta r = 1 \text{ mm} \ \& \ L = 5 \text{ mm}$				
	50 eV	100 eV	200 eV	1 keV
σ_1	0.235	0.161	0.111	0.047
σ_2	0.197	0.144	0.104	0.048
$\Delta r = 4 \text{ mm} \ \& \ L = 5 \text{ mm}$				
	50 eV	100 eV	200 eV	1 keV
σ_1	0.239	0.164	0.113	0.048
σ_2	0.199	0.145	0.105	0.049
$\Delta r = 4 \text{ mm} \ \& \ L = 0 \text{ mm}$				
	50 eV	100 eV	200 eV	1 keV
σ_1	0.241	0.166	0.116	0.051
σ_2	0.197	0.143	0.103	0.047

Table 3: Values of σ_1 and σ_2 for different studies and different recoil energies in the case of Point-like \ 3-D B.A.

5 S/N evaluation

The best achievable resolution must deal with the need to perform the calibration in a short time lapse. These two requirements often compete. Thus, it is necessary to find a balance between high rate and good precision.

In this context, an estimate of S/N is important in order to compare the different setup configurations in terms of time necessary to get the number of events (and the precision) that is required for the calibration.

The first step is to estimate the event rate with the help of simulation results and geometrical considerations. Then, an estimate of background rate is done, through preliminary studies with SiPMs.

5.1 Estimate of event rate

This first rough estimate includes geometrical considerations and probability of interaction inside of the target and the detector. For now, no considerations about detector efficiency and threshold influence were made, since studies of SiPM+scintillating fiber coupling are needed.

From the Monte Carlo simulation, the number of emitted neutrons that reach the target is obtained (starting from a total number of 10^{12} neutrons). The number of neutrons that effectively interact with the target is obtained multiplying by:

$$(1 - e^{-thickness/\lambda}) \tag{4}$$

Then, the number of particles that reach the B.A. is simply computed evaluating the fraction of solid angle covered by the detector. Lastly, the number of detected neutrons is given multiplying for the same factor (Eq.4), in which λ is the interaction length in the scintillating fibers (41.4 mm) and *thickness* is the length of the detector in the z-direction.

The results for the configuration setup with standard parameters and that with 6 mm collimator radius are shown in **Figure 9** for different recoil energies and Target-Detector distances.

5.2 Estimate of background rate: first studies with SiPMs

A Silicon PhotoMultiplier is a light detector employed in all those applications where low light/radiation levels must be measured and quantified with high precision. It is designed to have high gain and high detection efficiency so that even a single photon impinging on a SiPM pixel can be detected. The structure of a SiPM allows “parallel” photon detection, meaning that more photons can be detected at the same time enabling photon counting [3].

The basic structure of a SiPM consists of a matrix of small-sized sensitive elements called micro-cells (or pixels) all connected in parallel. Each micro-cell is a Geiger-Mode avalanche photo-diode (GM-APD) working beyond the breakdown voltage and it integrates a resistor for passive quenching (**Figure 10**).

If a SiPM absorbs a photon, the resulting charge carrier (an electron or hole depending on the structure) can trigger an avalanche in the gain region. The avalanche can produce $10^5 - 10^6$ carriers (the gain depends linearly on the overvoltage and the value of junction capacitance), and therefore a detectable current signal. The role of the quenching resistor is to restore the APD back to the Geiger mode.

The output is a time sequence of waveforms (or current pulses), which have a discrete distribution of amplitudes, since the output signals of the pixels are identical and N independent current

■ 100 cm
 ■ 150 cm
 ■ 200 cm
 ■ 300 cm

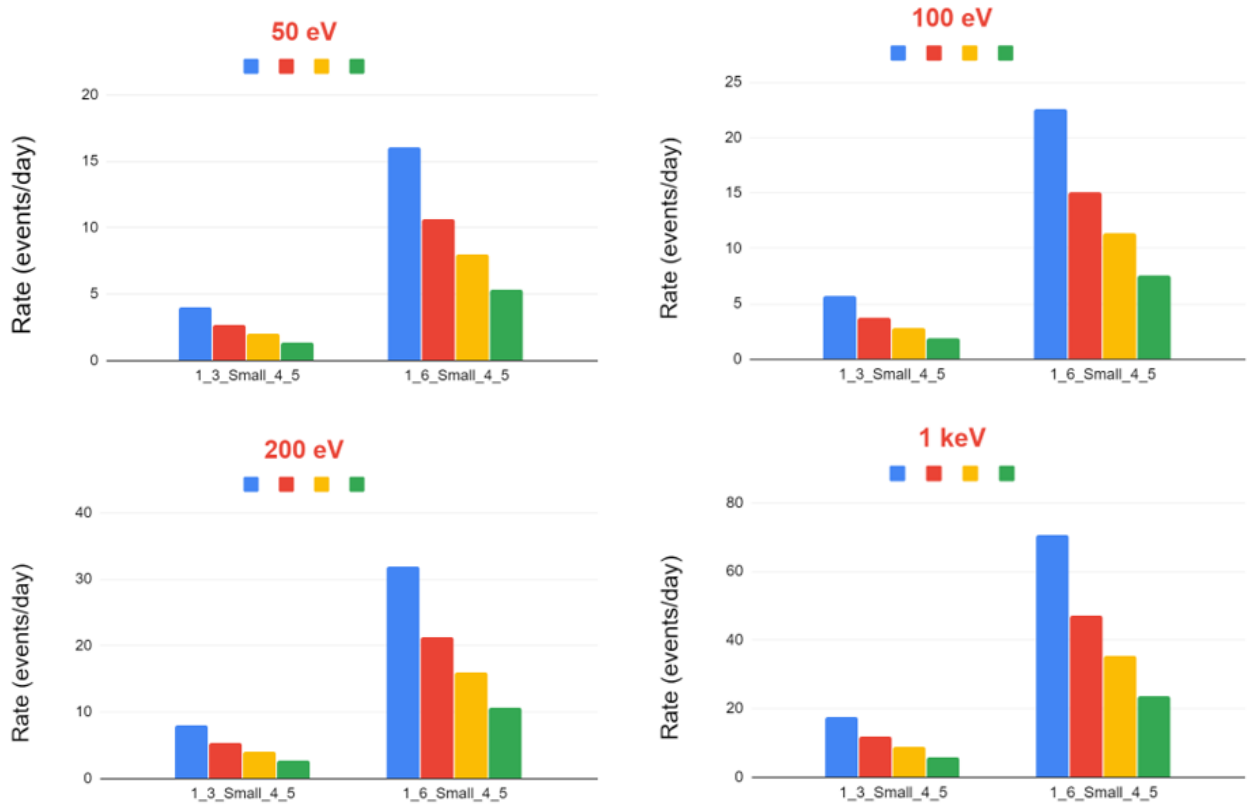


Figure 9: Rate in events per day in the configuration with default parameters and with 6 mm collimator radius. As the collimator radius doubles, the rate quadruples.

pulses coming from N different pixels just add up at the SiPM terminals.

Figure 11 shows a typical SiPM output seen at the oscilloscope. The peaks corresponding to 1,2,3,etc. photoelectrons (which means 1,2,3,etc. simultaneous firing pixels) are clearly visible. Most of them are probably not due to real events but to crosstalks. Optical crosstalk involves photons emitted during avalanche multiplication and that are re-absorbed in neighboring cells or even in the inactive region of the same cell and causing additional current pulses. Another type of correlated noise is the afterpulsing (also visible in **Figure 11**), which is due to the carriers trapped in silicon defects during the avalanche multiplication that are released later on during the recharge phase of the GM-APD.

In this work, two SiPMs (Hamamatsu model S12572-100C, 3 mm x 3 mm area, identified as "Blue" and "Yellow") are studied in order to measure the dark count rate of the single detector and of the coincidence of the two. They are placed inside a dark box, and can communicate with external devices (Oscilloscope, Digitizer, Computer) through an evaluation board (**Figure 12**).

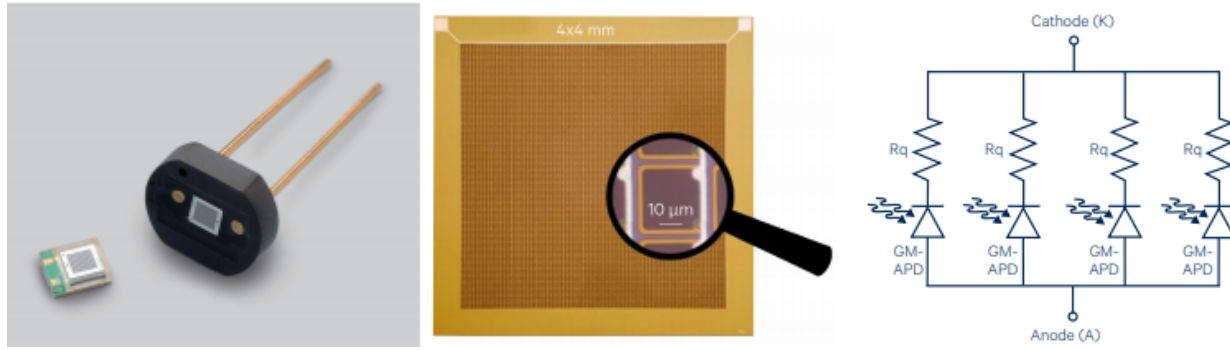


Figure 10: Structure of a SiPM.

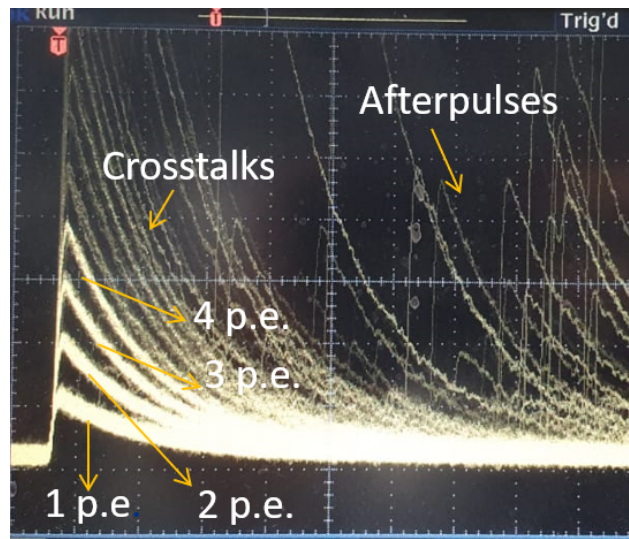


Figure 11: Oscilloscope trace with the display set to persistence mode.

The first step in this study deals with the measurement of the breakdown voltage of the two SiPMs. In order to extract it, the pulse height of 1 p.e. signal is measured at the oscilloscope for different bias voltages: the relationship is linear and the intercept with the y-axis of the interpolating line is the breakdown voltage (**Figure 13**).

This first measurement is important to find the appropriate operating voltage (the recommended one is $\sim V_{br} + 1V$). In principle the higher the overvoltage ($V_{br} - V_{bias}$), the higher the SiPM performances. In reality, since the detection efficiency tends to saturate with the overvoltage while the noise keeps on increasing (even more than linearly) there exists an upper limit to the optimum SiPM bias voltage.

At the same time, the knowledge of the relationship between pulse height of 1 p.e. and the bias voltage allows to impose threshold in terms of number of p.e., and this is crucial for the dark count

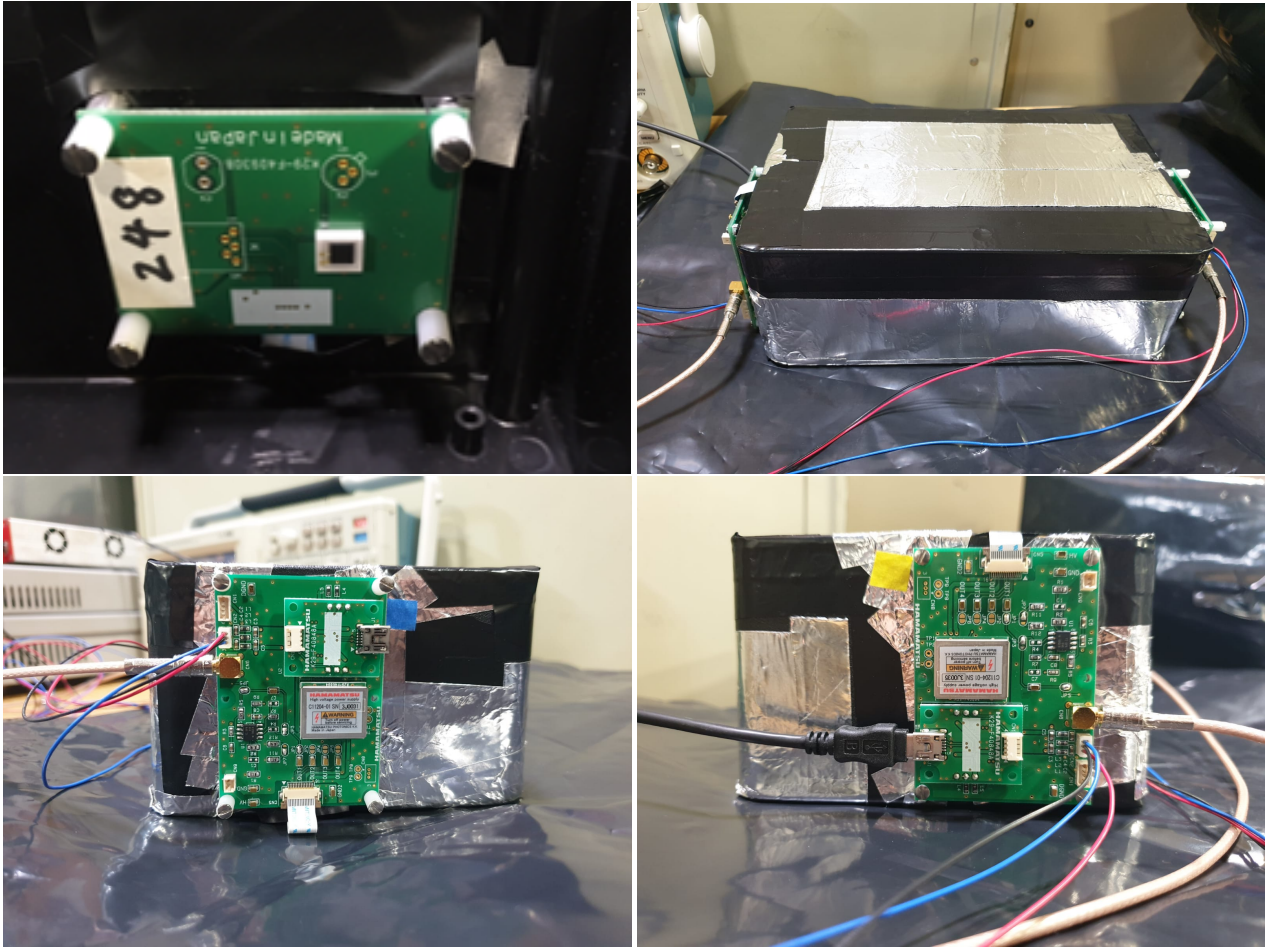


Figure 12: Top left: SiPM on the board, fixed into the dark box; Top right: dark box, well taped to avoid light leak; Bottom: evaluation boards of the two SiPMs, fixed at the outside of the dark box.

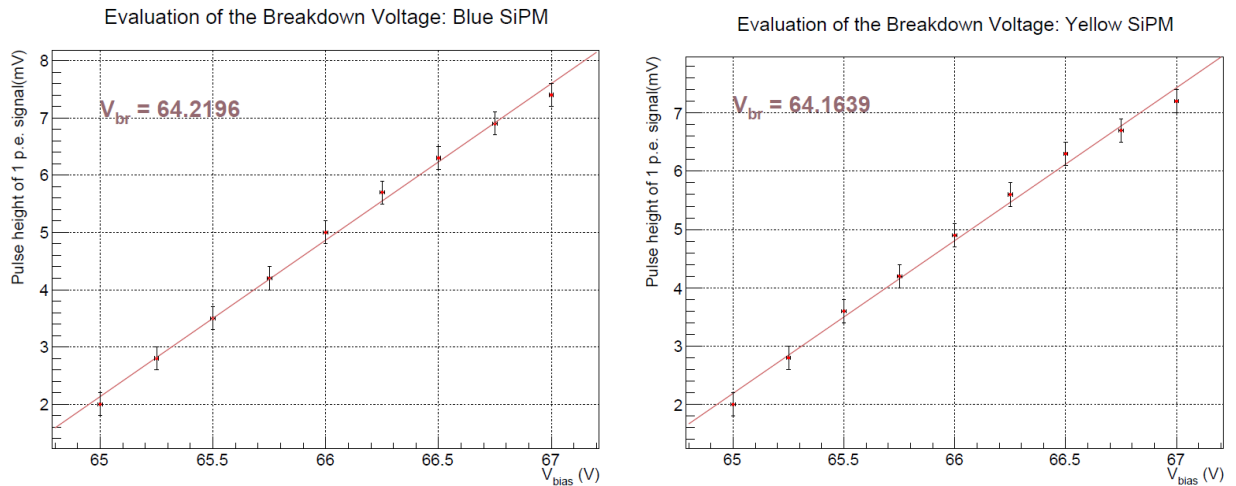


Figure 13: Pulse height of 1 p.e. signal as a function of the biasing voltage for the two SiPMs. V_{br} is the extrapolated breakdown voltage

rate measurement.

The dark counts are the primary source of noise in SiPMs: they are represented by spurious output current pulses produced in absence of light. A dark event happens when an e-h pair originates due to thermal agitation inside the active region of a GM-APD, an avalanche is initiated and an output pulse is observed. The number of dark events per unit time is the dark count rate (DCR), and it is an increasing function of the overvoltage, SiPM active area and temperature.

Figure 14 shows the setup for the dark count rate measurements: the dark box is covered by many layers of opaque black plastic, the temperature and the bias voltage are controlled, data are acquired and analyzed through Daqman software that communicates with the Digitizer.

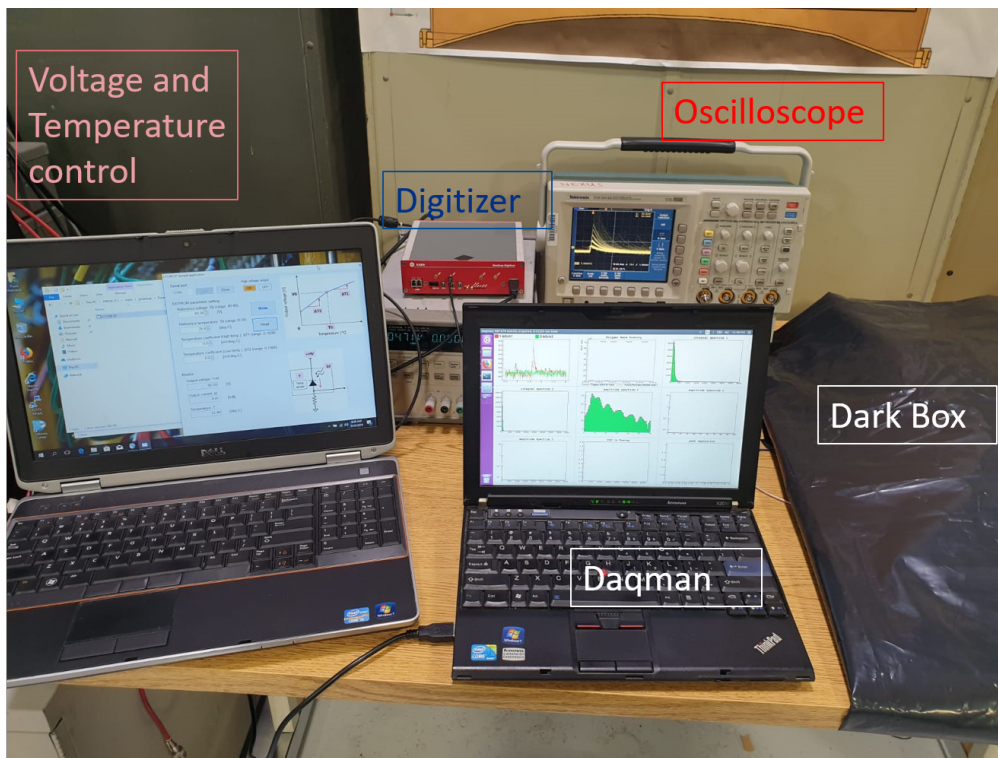


Figure 14: Setup for dark count rate measurements.

The measurement is performed taking the threshold at 3 p.e. for both SiPMs and the rate is evaluated for different values of bias voltage. The rate (**Figure 15**) in the small-overvoltage region is distorted, because the noise easily overcome the low threshold. However, except for this region, the rate increase with the bias voltage as expected and is consistent with the nominal value for this SiPM (considering that the high crosstalk probability for this model strongly affect the dark rate). Since in the final configuration of the detector, two SiPMs will be connected to the two ends of a scintillating fiber and their signals will be put in coincidence, the coincidence rate of Blue and Yellow SiPMs is measured as well (**Figure 16**). The bias voltage is fixed at 65 V, the coincidence window at 80 ns, and the threshold is changed from 1 to 3 p.e. (imposed on both SiPMs).

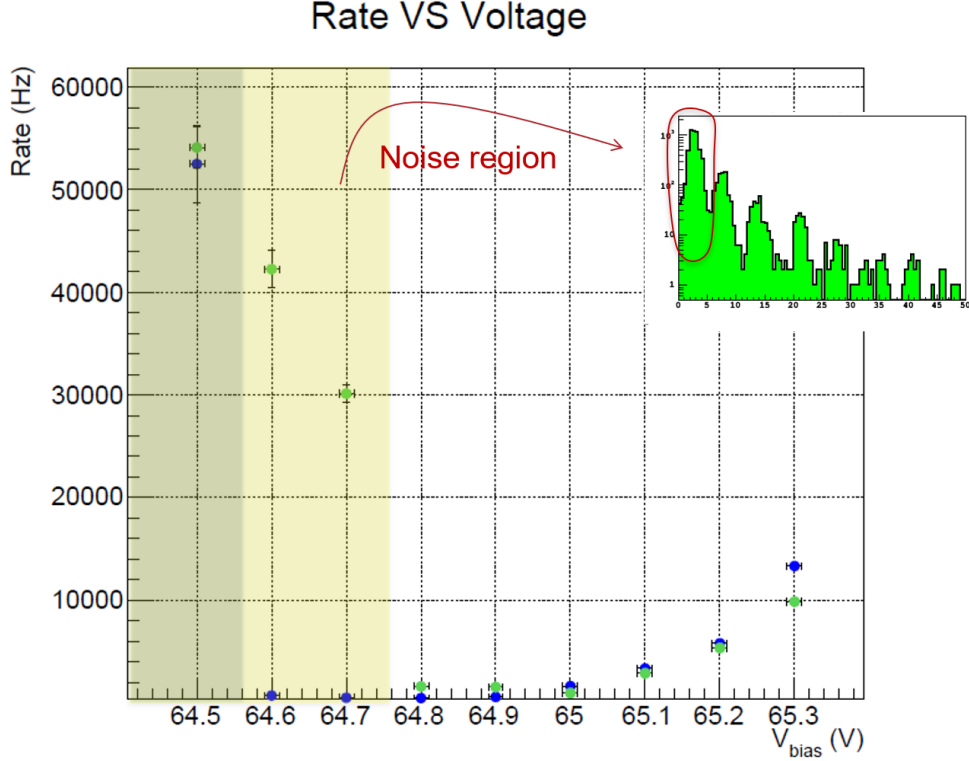


Figure 15: Rate versus bias voltage for Blue SiPM (blue marker) and Yellow one (green marker). The colored region is the noise region: as visible from the amplitude spectrum, a lot of events are not real dark events but just noise that overcome the imposed threshold.

This coincidence rate is not the actual background rate, since in the calibration experiment a signal from the B.A. will be accepted only if it is accompanied by a signal (a neutron scatter) in the SuperCDMS detector within a coincidence window of $10 \mu s$. Consequently, what matters is the accidental coincidence between the B.A. and the SuperCDMS detector. Moreover the Region Of Interest (ROI) for the experiment is between 50 eV and 1 keV, this means that the calibration experiment is not interested in energies from 1 keV up to the the maximum recoil in Si for an incident neutron of energy 2.45 MeV (~ 300 keV). Accordingly, the calculation is corrected for this factor.

Therefore, the background rate in coincidence with SuperCDMS detector in ROI in 3.3_Small configuration (3 mm source radius, 3 mm collimator radius, small SuperCDMS detector) is evaluated (**Figure 17**). Experimental points in **Figure 16** are multiplied for the interaction rate at target for the case 3.3_Small, for the coincidence window and for the energy window factor (which is ROI/Maximum energy $\sim 1/300$).

These results are compared to the event rate estimate for the same configuration (**Figure 18**). The dark rate represents a significant background for thresholds less than ~ 2 p.e. for the calibration measurement, since the rate is equal to or higher than the expected signal rate. It can be

observed that putting the backing array closer to the target is preferable even though the systematics calculated in the first half of the report suggest to place it further away. As usual, it is necessary to find a compromise, in this case probably represented by the 150 cm Target-Detector distance.

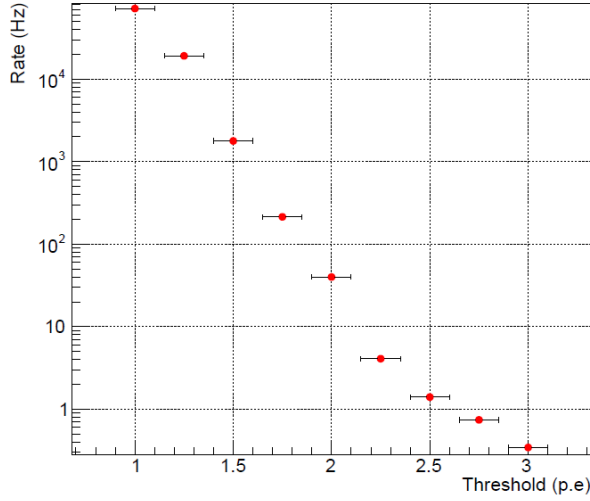


Figure 16: Coincidence rate at 65 V with 80 ns window.

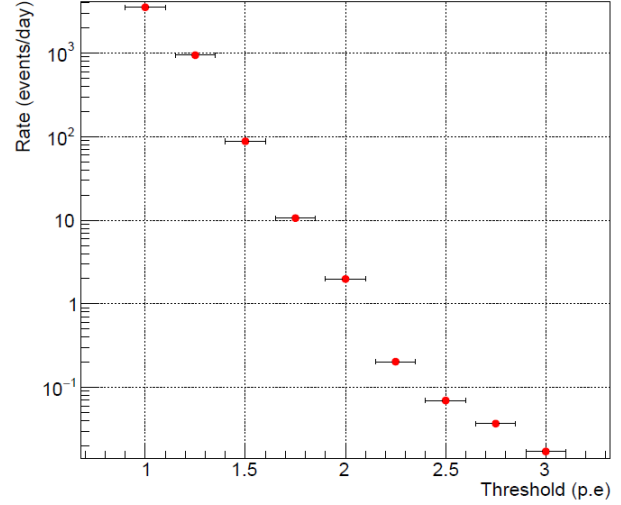


Figure 17: Background rate in coincidence with SuperCDMS detector in ROI in 3.3_Small configuration.

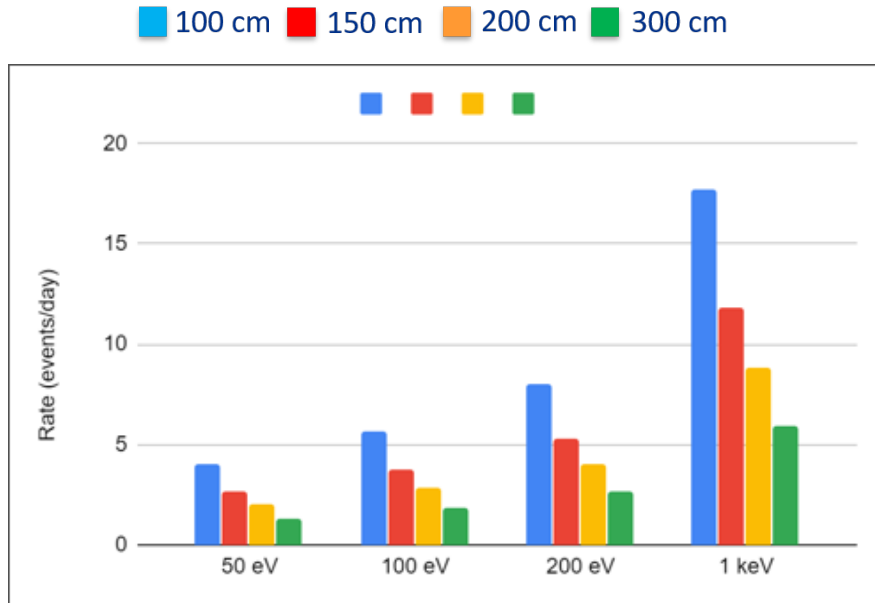


Figure 18: Event rate in 3.3_Small configuration.

6 Conclusion

This first study shows that dark counts represent a non negligible background in the calibration experiment. Studies with SiPMs coupled with scintillating fibers (**Figure 19**) are needed to understand the proper threshold to impose and then evaluate S/N for different thresholds and different sets of parameters.

Although the study is not complete, this work takes the first fundamental steps in the preliminary analysis to determine the best detector geometry that achieves a compromise between high precision and high rate.

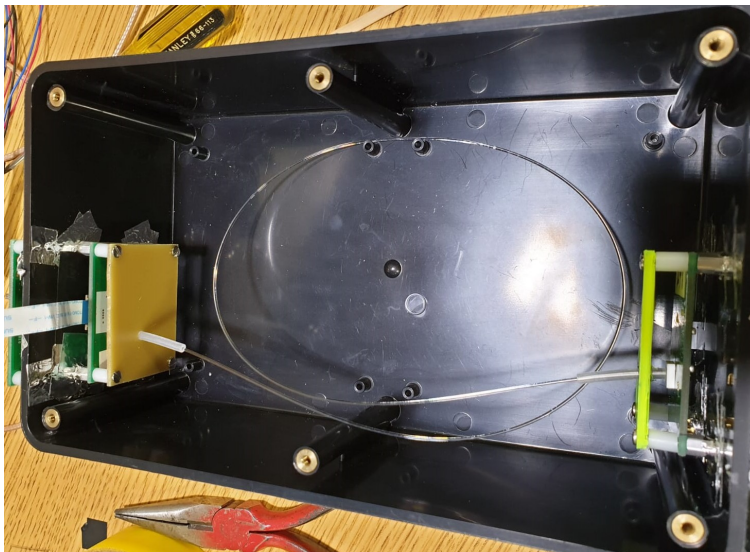


Figure 19: Scintillating fiber into the dark box coupled with two SiPMs at the ends.

Appendici

Appendix A Energy histograms

Every plot shows a $\Delta E/E$ histogram for a fixed recoil energy, at different values of Target-Detector distance (100 cm, 150 cm, 200 cm, 300 cm).

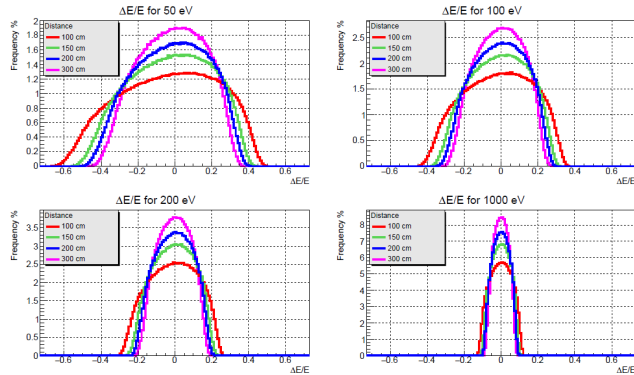


Figure 20: Default parameter

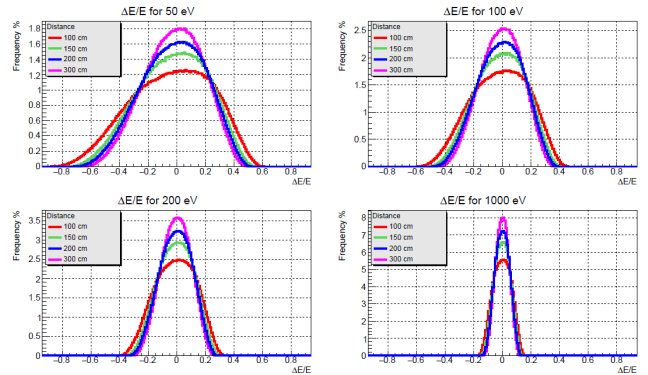


Figure 21: 3 mm source radius

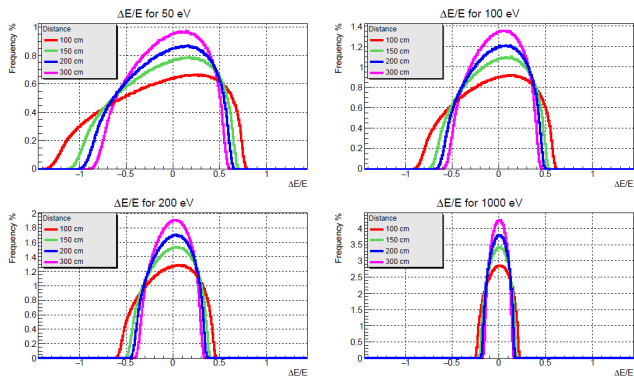


Figure 22: 6 mm collimator radius

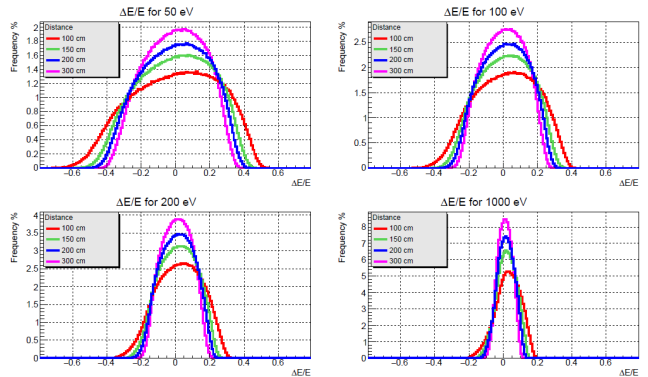


Figure 23: Big SuperCDMS detector

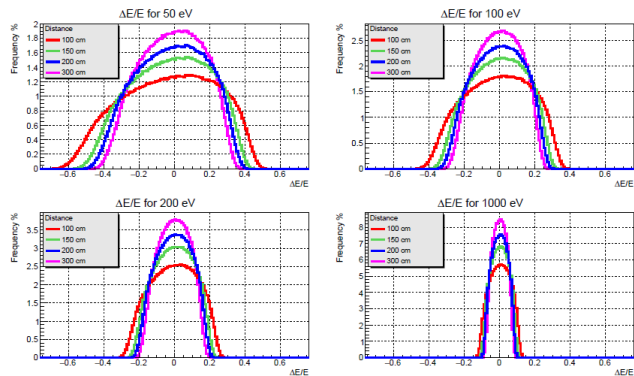


Figure 24: $\Delta r=1$ mm & $L=5$ mm

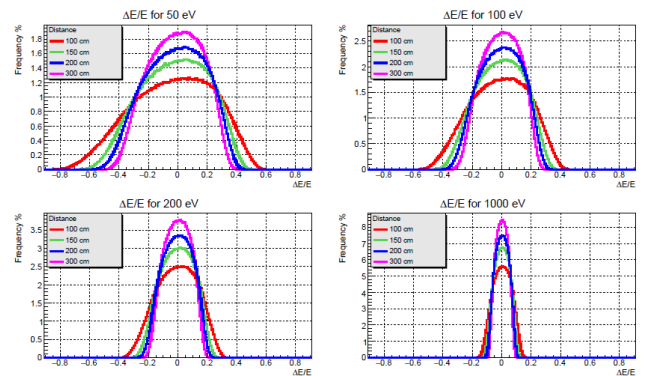


Figure 25: $\Delta r=4$ mm & $L=5$ mm

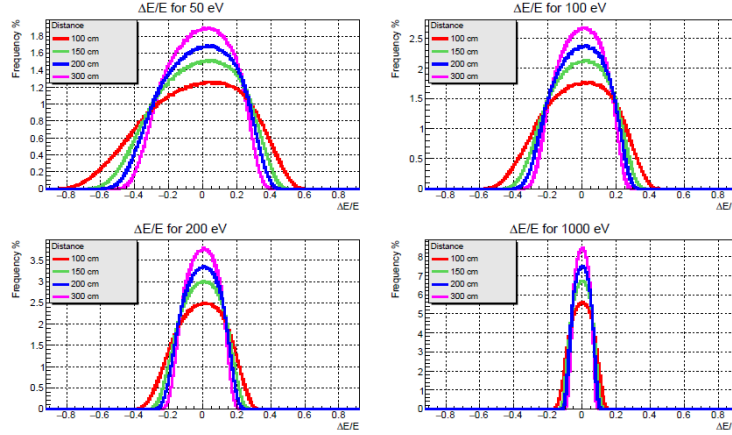


Figure 26: $\Delta r = 4$ mm & $L = 0$ mm

References

- [1] Izraelevitch, F., Amidei, D., Aprahamian, A., Arcos-Olalla, R., Cancelo, G., Casarella, C., ... & Guardincerri, Y. (2017). A measurement of the ionization efficiency of nuclear recoils in silicon. *Journal of Instrumentation*, 12(06), P06014.
- [2] Agnese, R., Anderson, A. J., Aramaki, T., Arnquist, I., Baker, W., Barker, D., ... & Brink, P. L. (2017). Projected Sensitivity of the SuperCDMS SNOLAB experiment. *Physical Review D*, 95(8), 082002.
- [3] Slawomir, P. (2016). What is an SiPM and how does it work?. Hamamatsu Corporation & New Jersey Institute of Technology. Taken from <https://hub.hamamatsu.com/jp/en/technical-note/how-sipm-works/index.html> .